AIP The Journal of Chemical Physics

An ab initio study of the electronic structure of boron arsenide, BAs

Ilias Magoulas and Apostolos Kalemos

Citation: J. Chem. Phys. **139**, 154309 (2013); doi: 10.1063/1.4824886
View online: http://dx.doi.org/10.1063/1.4824886
View Table of Contents: http://jcp.aip.org/resource/1/JCPSA6/v139/i15
Published by the AIP Publishing LLC.

THE JOURNAL OF CHEMICAL PHYSICS **139**, 154309 (2013)

An *ab initio* study of the electronic structure of boron arsenide, BAs

Ilias Magoulas and Apostolos Kalemos[a]

Laboratory of Physical Chemistry, Department of Chemistry, National and Kapodistrian University of Athens, Panepistimiopolis, Athens 15771, Greece

(Received 15 April 2013; accepted 27 September 2013; published online 17 October 2013)

The completely unexplored BAs diatomic has been thoroughly studied by high level multireference variational *ab initio* methods. Potential energy curves for 42 molecular states dissociating to the first four asymptotic channels and covering an energy range of 5.8 eV have been constructed revealing an interesting morphology and a rich spectroscopy. The ground state is of $^3\Pi$ symmetry while its first excited $^1\Sigma^+$ state lies ~8 kcal/mol higher. A general feature of the potential curves is the presence of avoided crossings that challenge the validity of the Born Oppenheimer approximation. © *2013 AIP Publishing LLC*. [http://dx.doi.org/10.1063/1.4824886]

I. INTRODUCTION

Boron arsenide (BAs), isovalent to boron nitride (BN) and boron phosphide (BP), is a rather simple diatomic species but at the same time completely unknown from both a theoretical and experimental points of view.

The first study ever on BAs appeared as a short communication in Acta Crystallographica in 1958.[1] It is therein reported that it crystallizes with the cubic zinc blende structure with a lattice constant of 4.777 Å while its unit cell (c-face centered) is characterized by the $\alpha = 9.710$, $b = 4.343$, and $c = 3.066$ Å parameters. It is also stable when heated in the presence of arsenic vapor up to 920 °C while above this temperature it is transformed irreversibly into a tan colored orthorhombic structure.

Since then numerous properties of solid state BAs have been reported[2] but we could not trace even a single work on the diatomic BAs molecule even at the Hartree–Fock (HF) level of theory. On the contrary, there are several detailed studies on both the BN[3] and BP[3(d),4] diatomics. The ground state of the BN system is of $^3\Pi$ symmetry with its first excited $^1\Sigma^+$ state lying only a few wavenumbers above; 94.4 cm^{-1},[3(c)] 183 ± 40 cm^{-1},[3(e)] and 111.5 or 134.3 cm^{-1},[3(h)] while the experimental value is 158 ± 36 cm^{-1}.[5] In both the $X\ ^3\Pi$ and $a\ ^1\Sigma^+$ states the *in situ* B atom is in its excited $^4\mathrm{P}(2\mathrm{s}^1 2\mathrm{p}^2)$ state thus the maximum number of bonds between the $\mathrm{N}(^4\mathrm{S}_u)$ and $\mathrm{B}(^4\mathrm{P}_g)$ atoms are formed, i.e., $(1\sigma, 1\frac{1}{2}\pi)$ and $(1\sigma, 2\pi)$ for the $X\ ^3\Pi$ and $a\ ^1\Sigma^+$ states, respectively.[3(c)]

BP behaves similarly, i.e., its ground state is of $^3\Pi$ symmetry and its first excited state of $^1\Sigma^+$ symmetry but their energy gap $\Delta\mathrm{E}(a\,^1\Sigma^+ \leftarrow X\ ^3\Pi) \approx 8$ kcal/mol[3(d)] is much larger than the corresponding one in the BN molecule. Although the adiabatic dissociation limit of the BP $a\,^1\Sigma^+$ state $[\mathrm{P}(^2\mathrm{D}_u) + \mathrm{B}(^2\mathrm{P}_u)]$ lies closer to its ground state fragments, $\mathrm{P}(^4\mathrm{S}_u) + \mathrm{B}(^2\mathrm{P}_u)$, than it happens in the BN case; $\Delta\mathrm{E}_{\mathrm{N/P}}\ (^2\mathrm{D}_u \leftarrow {}^4\mathrm{S}_u) = 2.38/1.41$ eV,[6] the internal bond strength of the $a\ ^1\Sigma^+$ state is weaker in BP than in BN due perhaps to the different size of the P and N atoms; $\langle r_{3p}\rangle_P / \langle r_{2p}\rangle_N = 1.65$.[7]

The complete lack of any knowledge on the diatomic BAs molecule prompted the present work with the belief that it will be an impetus for its spectroscopic investigation in the near future. To this end, we have constructed potential energy curves (PEC) for all states originating from the first four asymptotic channels, i.e., $\mathrm{B}(2\mathrm{s}^2 2\mathrm{p}^1;\ ^2\mathrm{P}) + [\mathrm{As}(4\mathrm{s}^2 4\mathrm{p}^3;\ ^4\mathrm{S}),\ \mathrm{As}(4\mathrm{s}^2 4\mathrm{p}^3;\ ^2\mathrm{D}),\ \mathrm{As}(4\mathrm{s}^2 4\mathrm{p}^3;\ ^2\mathrm{P})]$ and $\mathrm{B}(2\mathrm{s}^1 2\mathrm{p}^2;\ ^4\mathrm{P}) + \mathrm{As}(4\mathrm{s}^2 4\mathrm{p}^3;\ ^4\mathrm{S})$ based on high level multireference configuration interaction (MRCI) calculations.

II. COMPUTATIONAL DETAILS

For the description of both B and As we have employed the Dunning correlation consistent polarized valence quintuple zeta (cc−pV5Z) basis set $(14s8p4d3f2g1h/_{\mathrm{B}}$[8(a)] $26s17p13d3f2g1h/_{\mathrm{As}}$[8(b)]$)$ generally contracted to $[6s5p4d3f2g1h/_{\mathrm{B}}\ 8s7p5d3f2g1h/_{\mathrm{As}}]$ comprising a total of 195 spherical gaussian functions. For scalar relativistic calculations the cc−pV5Z−DK basis set has been used that takes into account the contraction scheme suggested by de Jong *et al.*[8(c)]

Our reference wavefunction is of the complete active space self consistent field (CASSCF) type and results from the distribution of 6 $(2\mathrm{s}^2 2\mathrm{p}^1/_{\mathrm{B}} + 4\mathrm{p}^3/_{\mathrm{As}})$ valence electrons among 7 $(2\mathrm{s}{+}2\mathrm{p}(3)/_{\mathrm{B}} + 4\mathrm{p}(3)/_{\mathrm{As}})$ orbitals. States of the same spin and spatial $(\Lambda^{\pm})$ symmetry originating from the first four asymptotic channels were considered simultaneously in a state average, SACASSCF, optimization procedure. Dynamical correlation was extracted by considering single and double replacements of 8 valence electrons out of all configuration functions (CF) of our zeroth order wavefunction. The MRCI space comprises of 1.4×10^6 $(^7\Sigma^+)$ to 1.7×10^7 $(^3\Pi)$ CFs internally contracted to 2×10^5 to 2×10^6 CFs, respectively. Size non-extensivity errors amount to approximately 4–5 $m\mathrm{E}_h$ and are practically nullified at the MRCI+Q (+Q = Davidson correction) level of theory.

All calculations were performed under C_{2v} symmetry and equivalence restrictions by the MOLPRO 2010.1 program.[9]

---

[a] kalemos@chem.uoa.gr

0021-9606/2013/139(15)/154309/11/$30.00

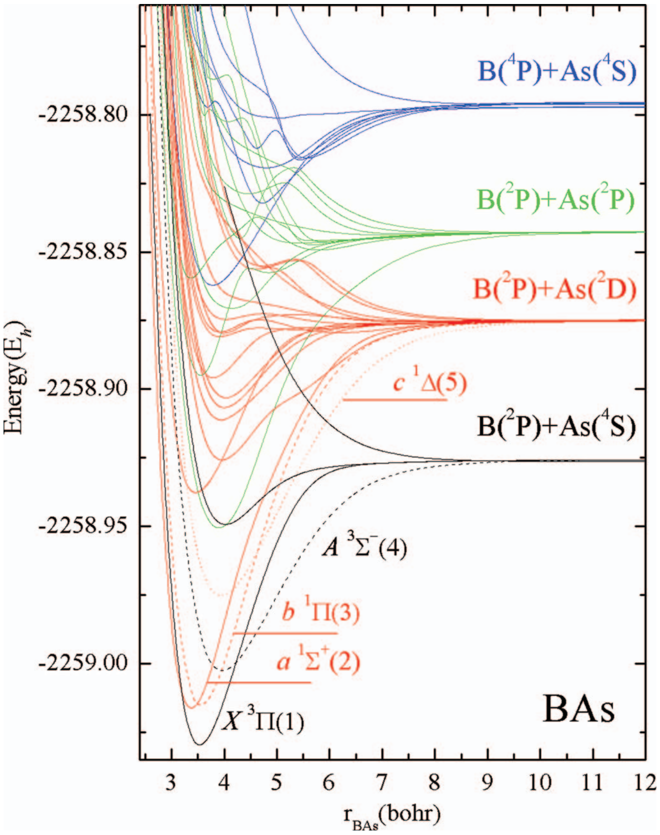

FIG. 1. Potential energy curves of all 42 BAs states presently studied at the MRCI/cc−pV5Z level of theory.

III. RESULTS AND DISCUSSION

Figure 1 displays PECs of all 42 molecular $^{2S+1}\Lambda^{\pm}$ states resulting from the first four asymptotic channels, namely B(^{2}P) + As(^{4}S) → BAs $^{3,5}(\Sigma^-, \Pi)$, B(^{2}P) + As(^{2}D) → BAs $^{1,3}(\Sigma^+, \Sigma^-[2], \Pi[3], \Delta[2], \Phi)$, B(^{2}P) + As(^{2}P) → BAs $^{1,3}(\Sigma^+[2], \Sigma^-, \Pi[2], \Delta)$, and B(^{4}P) + As(^{4}S) → BAs $^{1,3,5,7}(\Sigma^+, \Pi)$, lying 1.379(1.318) [1.337] [*B*(^{2}*P*) + *As*(^{2}*D*)], 2.254(2.221)[2.293] [*B*(^{2}*P*) + *As*(^{2}*P*)], and 3.598(3.628) [3.551] [*B*(^{4}*P*) + *As*(^{4}*S*)] eV above the ground state fragments [B(^{2}P) + As(^{4}S)] at the MRCI(+Q)[expt][6] level, while Table I presents numerical results for 33 states; the rest (42 – 33 = 9) being of purely repulsive nature. Molecular states of the same and/or similar symmetry properties are grouped together and displayed in Figures 2–6 for reasons of convenience, analysis and discussion of their topology. In what follows, we tag the molecular states by a letter alluding to the standard spectroscopic notation and by a number referring to its ascending energy order.

A. *X* $^3\Pi$(1), *C* $^3\Pi$(9), *D* $^3\Pi$(10), *E* $^3\Phi$(11), *H* $^3\Pi$(16), *J* $^3\Pi$(19), *N* $^3\Pi$(29), and *O* $^3\Pi$(31)

The *X*, *C*, *D*, *H*, *J*, *N*, and *O* $^3\Pi$ states correlate adiabatically to B(^{2}P, M$_L$ = ±1) + As(^{4}S), B(^{2}P, M$_L$ = ±1) + As(^{2}D, M$_L$ = 0), B(^{2}P, M$_L$ = ±1) + As(^{2}D, M$_L$ = ∓ 2), B(^{2}P, M$_L$ = 0) + As(^{2}D, M$_L$ = ±1), B(^{2}P, M$_L$ = ±1) + As(^{2}P, M$_L$ = 0), B(^{2}P, M$_L$ = 0) + As(^{2}P, M$_L$ = ±1), and B(^{4}P, M$_L$ = ±1) + As(^{4}S), respectively, while the only state of $^3\Phi$ symmetry originates from the B(^{2}P, M$_L$ = ±1) + As(^{2}D, M$_L$ = ±2) asymptotic interaction; see Fig. 2.

The *X* state of the BAs species is of $^3\Pi$ symmetry in line with the isovalent BN[3] and BP[4] molecules. The main CASSCF equilibrium configuration and Mulliken atomic distributions (counting only valence orbitals)

$$|X^3\Pi(1)\rangle \approx 0.92\left|1\sigma^2 2\sigma^2 3\sigma^1 1\pi_x^1 1\pi_y^2\right\rangle$$

with 1σ ~ (0.91)4s$^{\mathrm{As}}$ + (0.30)2s$^{\mathrm{B}}$ + (0.21)2p$_z{}^{\mathrm{B}}$, 2σ ~ (0.72)2s$^{\mathrm{B}}$ + (0.21)2p$_z{}^{\mathrm{B}}$ – (0.65)4p$_z{}^{\mathrm{As}}$ – (0.36)4s$^{\mathrm{As}}$, 3σ ~ (0.55)2s$^{\mathrm{B}}$ – (0.72)2p$_z{}^{\mathrm{B}}$ – (0.54)4p$_z{}^{\mathrm{As}}$, and 1π ~ (0.39)2p$_\pi{}^{\mathrm{B}}$ + (0.86)4p$_\pi{}^{\mathrm{As}}$ and

$$2s^{1.40}2p_z^{0.65}2p_x^{0.30}2p_y^{0.64}(3d)^{0.08}/_B$$

$$4s^{1.76}4p_z^{1.04}4p_x^{0.70}4p_y^{1.29}(4d)^{0.11}/_{As},\ q_B = -0.07$$

reveal an *in situ* B atom excited in its ^{4}P state while the bonding situation can be nicely described by the following valence bond Lewis (vbL) diagram:

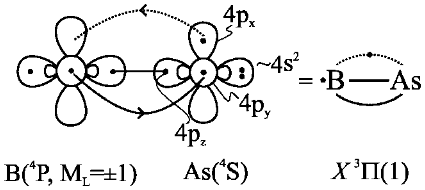

showing a σ, a full and a half π bonds. The atomic populations, providing a bonding tendency than a definitive state of affairs, show a rather intense charge transfer of 0.30e$^-$ along the π_x and π_y frames but of opposite directions, thus the total charge on the atomic centers is close to zero. The equilibrium distance is found at r$_e$ = 1.869 (1.870) [1.866] Å with a binding energy value of D$_e$ = 65.24(66.3)[64.50] kcal/mol at the MRCI(+Q) [RCCSD(T)] levels of theory. Scalar relativistic effects computed at the MRCI(+Q)[RCCSD(T)]−DKH2/cc−pV5Z−DK level of theory contribute extremely very little to the bonding characteristics; r$_e$ = 1.864(1.867)[1.862] Å and D$_e$ = 64.37(65.2)[64.12] kcal/mol. By considering also the diagonal spin–orbit effects we found that the Ω = 2 and Ω = 0$^\pm$ states are translated by ∓390 cm^{-1} (1.12 kcal/mol) with respect to the Ω = 1 state with identical to the *X* $^3\Pi$ state's spectroscopic constants. No core–valence correlation effects were considered due to the huge number (2 + 18 = 20) of core electrons. Its dipole moment expectation value is rather small, $\langle\mu\rangle$ = 0.20 D, while when calculated by the finite field approach it is close to zero, μ_{ff} = 0.07 D, in remarkable similarity with the value of the *X* $^3\Pi$ state of the BP molecular species, μ_0 = 0.06 D,[4(c)] but in disaccord with the large value of μ = 1.948 D of the BN *X*-state.[3(c)]

The next three states of $^3\Pi$ symmetry, namely the *C*, *D*, and *H*, although they correlate adiabatically to B(^{2}P, M$_L$ = ±1,±1,0) + As(^{2}D, M$_L$ = 0, ∓ 2,±1), respectively, they are characterized by an intense mixing with the B(^{4}P) atomic state as evidenced by the Mulliken analysis (*vide infra*) and the morphology of the PECs (see Fig. 2).

The main CASSCF equilibrium configurations and Mulliken atomic populations of the *C* and *D* states

TABLE I. Energies E (E_h), bond distances r_e (Å), dissociation energies D_e (kcal/mol), harmonic frequencies ω_e (cm^{-1}), anharmonic corrections $\omega_e x_e$ (cm^{-1}), dipole moments μ (D), and energy gaps T_e (kcal/mol) of thirty three $^{11}B^{75}As$ states at the MRCI(+Q)[RCCSD(T)]/cc−pV5Z level of theory.

State	$-E$	r_e	D_e[a]	ω_e	$\omega_e x_e$	$\langle\mu\rangle/\mu_{ff}$[b]	T_e
$X^3\Pi(1)$	2259.02978	1.869	65.24	792.0	8.00	0.20/0.07	0.0
	(2259.0418)	(1.870)	(66.3)	(776.6)	(3.53)	/0.09	0.0
	[2259.037 52]	[1.866]	[64.50]	[789.5]	[5.02]		0.0
$a^1\Sigma^+(2)$	2259.01627	1.788	88.53	874.1	5.28	−0.25/−0.13	8.5
	(2259.029 6)	(1.788)	(88.7)	(870.1)	(3.89)	/−0.13	(7.7)
$b\ ^1\Pi(3)$	2259.01517	1.879	87.86	772.8	3.54	−0.03/−0.04	9.2
	(2259.028 7)	(1.878)	(88.1)	(777.1)	(3.55)	/−0.02	(8.2)
$A^3\Sigma^-(4)$	2259.00273	2.094	48.31	538.6	3.88	1.33/ 0.59	17.0
	(2259.0159)	(2.092)	(50.1)	(530.3)	(2.98)	/0.61	(16.3)
$c^1\Delta(5)$	2258.97542	2.089	62.90	539.3	1.64	1.86/0.71	34.1
	(2258.9906)	(2.086)	(64.2)	(552.9)	(4.30)	/0.71	(32.1)
$d^1\Sigma^+(6)$	2258.95066	2.056	67.63	595.4	− 1.29	2.07/	49.6
	(2258.9645)	(2.063)	(69.0)	(609.0)	(0.08)		(48.5)
$e^5\Pi(7)$	2258.94986	2.111	15.14	479.8	7.89	0.92/	50.2
	(2258.9615)	(2.111)	(16.2)	(479.4)	(8.38)		(50.4)
$B^3\Sigma^+(8)$	2258.93793	1.826	39.55	659.4	5.77	0.66/	57.6
	(2258.950 0)	(1.830)	(38.9)	(658.2)	(5.66)		(57.6)
$C\ ^3\Pi(9)$	2258.92606	2.100	32.04	535.3	5.18	0.67/	65.1
	(2258.9393)	(2.105)	(32.3)	(526.6)	(5.25)		(64.3)
$D\ ^3\Pi(10)$	2258.91135	2.090	22.89	485.6	8.84	1.52/	74.3
	(2258.9253)	(2.094)	(23.5)	(482.5)	(8.06)		(73.1)
$E\ ^3\Phi(11)$	2258.90702	2.119	20.18	506.2	6.07	0.69/	84.6
	(2258.9218)	(2.119)	(21.2)	(501.8)	(5.88)		(75.3)
$f^1\Pi(12)$	2258.90326	2.132	17.64	488.9	7.14	0.736/	79.4
	(2258.9191)	(2.154)	(19.4)	(474.4)	(4.54)		(77.0)
$F^3\Delta(13)$	2258.89620	2.009	13.36	561.2	10.36	−0.23/	83.8
$G^3\Sigma^+(14)$	2258.89538	1.878	33.05	883.8	7.52	0.10/	84.3
(Local minimum)							
	2258.857 8	2.561		334.83	4.79		
$g^1\Sigma^-(15)$	2258.88129	2.053	3.89	392.5	22.22	−0.53/	93.2
	(2258.8988)	(2.052)	(6.7)	(455.1)	(27.14)		(89.7)
(Local minimum)							
	2258.87827	2.840		97.70	7.50		
$H^3\Pi(16)$	2258.87982	2.117	3.13	509.8	16.77	0.81/	94.1
	(2258.893 5)	(2.117)	(3.4)	(495.4)	(17.63)		(93.1)
$I^3\Sigma^-(17)$	2258.87941	3.281	2.81	112.9	1.73	0.21/	94.36
	(2258.8935)	(3.207)	(3.4)				(93.1)
(Local minimum)							
	2258.87925	2.072		440.9	17.12		
	(2258.8948)	(2.066)		(440.2)	(18.00)		
$h^1\Delta(18)$	2258.87621	3.556	0.71	55.7	4.20	0.21/	96.4
	(2258.8900)	(3.320)	(1.1)	(69.4)	(3.10)		(95.3)
(Local minimum)							
	2258.87458	2.133		305.3	10.06		
	(2258.8912)	(2.094)		(393.9)	(21.52)		
$J^3\Pi(19)$	2258.87075	2.198	17.61	354.0	− 5.33	0.50/	99.8
	(2258.887 0)	(2.178)	(20.6)	(374.5)	(− 6.37)		(97.1)
$i^5\Sigma^+(20)$	2258.86227	1.998	40.85	536.9	4.25	1.58/	105.1
	(2258.872 2)	(2.001)	(42.9)	(529.4)	(4.12)		(106.4)
$j\ ^1\Sigma^+(21)$	2258.85945	1.767	10.41	842.4	31.48	−0.34/	106.9
	(2258.877 7)	(1.789)	(14.5)	(823.7)	(28.44)		(103.0)
(Local minimum)							
	2258.84932	3.058		198.7	6.27		
	(2258.8637)	(2.996)		(220.0)	(3.76)		
$k^1\Sigma^-(22)$	2258.85661	2.421		348.7	15.19	2.01/	108.7
	(2258.875 3)	(2.352)		(426.1)	(13.47)		(104.5)

TABLE I. (*Continued.*)

State	−E	r_e	D_e[a]	ω_e	$\omega_e x_e$	$\langle\mu\rangle/\mu_{ff}$[b]	T_e
$K^3\Delta(23)$	2258.85535	2.492		313.7	10.29	2.23/	109.5
	(2258.8723)	(2.439)		(404.9)	(14.93)		(106.4)
$L^3\Delta(24)$	2258.84767	2.979	3.15	326.60	11.21	0.54/	114.3
$l^1\Delta(25)$	2258.84670	2.852	2.4	140.1	9.89	0.72/	114.9
$M^3\Sigma^+(26)$	2258.84655	2.276	2.45	901.2	22.22	1.40/	115.0
$m^1\Sigma^-(27)$	2258.84649	3.114	2.3	251.5	18.22	0.26/	115.0
$n^1\Sigma^+(28)$	2258.83311	2.491	23.67	688.0	30.02	0.61/	123.4
$N^3\Pi(29)$	2258.82894	2.356		299.9	− 1.35	− 0.18/	126.0
	(2258.846 2)	(2.289)		(307.1)	(3.21)		(122.7)
$o^5\Pi(30)$	2258.81946	2.542	14.73	270.5	1.20	0.92/	132.0
	(2258.8308)	(2.496)	(17.5)	(247.31)	(− 2.65)		(132.4)
$O^3\Pi(31)$	2258.81721	2.836	13.6	498.6	17.10	0.03/	133.4
$P^3\Sigma^+(32)$	2258.81671	2.858	13.40	618.3	32.33	1.07/	133.7
$p^1\Pi(33)$	2258.81619	2.928	12.90	403.5	11.30	− 0.20/	134.0
	(2258.829 6)	(2.866)	(16.7)	(444.1)	(11.12)		(133.2)

[a] Dissociation energies are given with respect to the adiabatic products.

[b] μ_{ff} is calculated by the finite field approach, field strength ranges from -5×10^{-5} to $+5\times10^{-5}$ a.u. In classical electrostatics the dipole moment vector points to the positive charge and the **E**-field lines (in dipoles or otherwise) point from the positive charge. The origin is on the center of mass with the As atom along the positive z axis.

are

$$|C^3\Pi(9)\rangle \approx \big|1\sigma^2 2\sigma^2 3\sigma^1\big[(0.71)1\bar{\pi}_x^1 1\pi_y^1 2\pi_y^1 + (0.46)1\pi_y^2 2\pi_x^1 - (0.41)1\pi_x^1 1\pi_y^1 2\bar{\pi}_y^1\big]\big\rangle$$

and

$$|D^3\Pi(10)\rangle \approx |1\sigma^2 2\sigma^2 3\sigma^1\big[(0.57)1\pi_x^1 1\bar{\pi}_y^1 2\pi_y^1 + (0.44)1\bar{\pi}_x^1 1\pi_y^1 2\pi_y^1 + (0.31)1\pi_x^1 1\pi_y^1 2\bar{\pi}_y^1 - (0.30)2\pi_x^1 1\pi_y^2\big]\big\rangle - 0.40\big|1\sigma^2 2\sigma^1 3\sigma^2 1\pi_x^1 1\pi_y^2\big\rangle,$$

where $1\sigma \sim (0.96)4s^{As} + (0.16)2s^B + (0.13)2p_z{}^B$, $2\sigma \sim (0.76)2s^B + (0.20)2p_z{}^B - (0.24)4s^{As} - (0.58)4p_z{}^{As}$, $3\sigma \sim (0.58)2s^B - (0.63)2p_z{}^B + (0.59)4p_z{}^{As}$, $1\pi \sim (0.89)4p_\pi{}^{As} + (0.29)2p_\pi{}^B$, and $2\pi \sim (0.92)2p_\pi{}^B - (0.42)4p_\pi{}^{As}$ and

$$2s^{1.41}2p_z^{0.61}2p_x^{0.32}2p_y^{0.74}(3d)^{0.06}/_B$$

$$4s^{1.84}4p_z^{1.0}4p_x^{0.74}4p_y^{1.15}(4d)^{0.12}/_{As},\ q_B = -0.14,$$

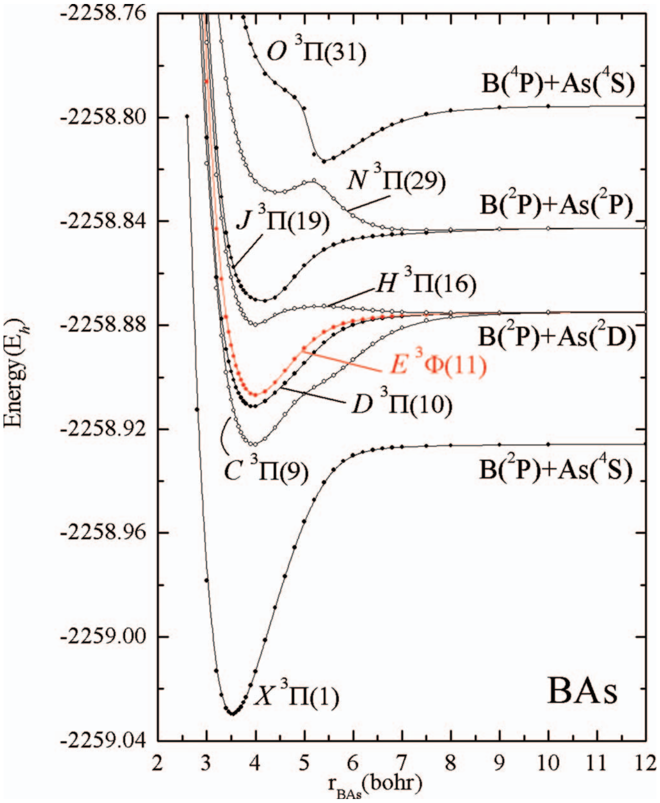

FIG. 2. MRCI/cc−pV5Z potential energy curves of the $X\ ^3\Pi(1)$, $C\ ^3\Pi(9)$, $D\ ^3\Pi(10)$, $E\ ^3\Phi(11)$, $H\ ^3\Pi(16)$, $J\ ^3\Pi(19)$, $N\ ^3\Pi(29)$, and $O\ ^3\Pi(31)$ states.

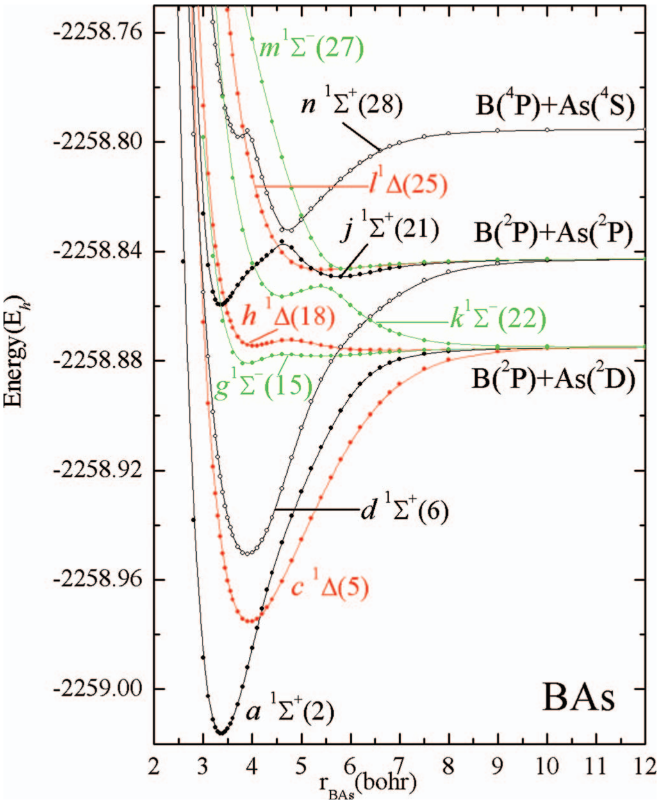

FIG. 3. MRCI/cc−pV5Z potential energy curves of $a\ ^1\Sigma^+(2)$, $c\ ^1\Delta(5)$, $d\ ^1\Sigma^+(6)$, $g\ ^1\Sigma^-(15)$, $h\ ^1\Delta(18)$, $j\ ^1\Sigma^+(21)$, $k\ ^1\Sigma^-(22)$, $l\ ^1\Delta(25)$, $m\ ^1\Sigma^-(27)$, and $n\ ^1\Sigma^+(28)$ states.

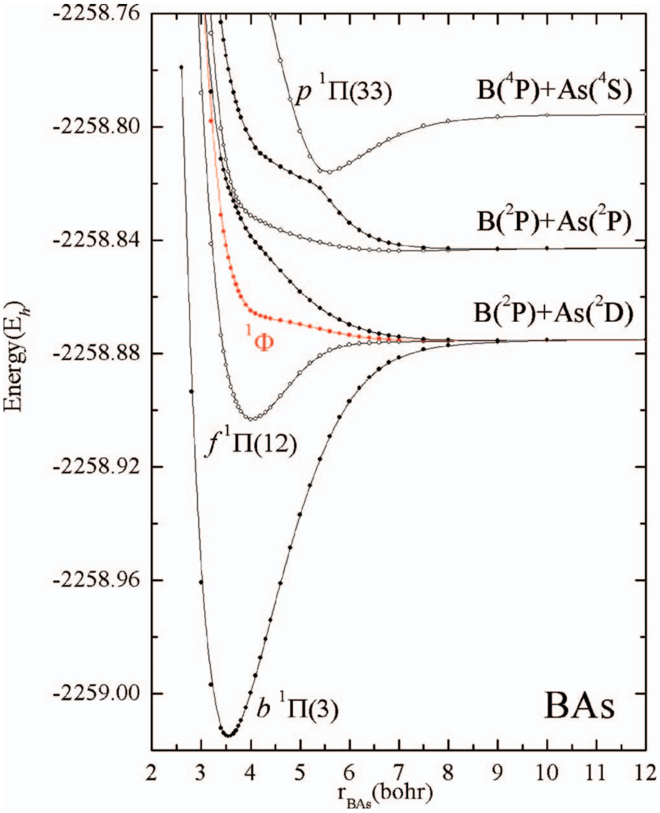

FIG. 4. MRCI/cc−pV5Z potential energy curves of the $b\ ^1\Pi(3)$, $f\ ^1\Pi(12)$, and $p\ ^1\Pi(33)$ states.

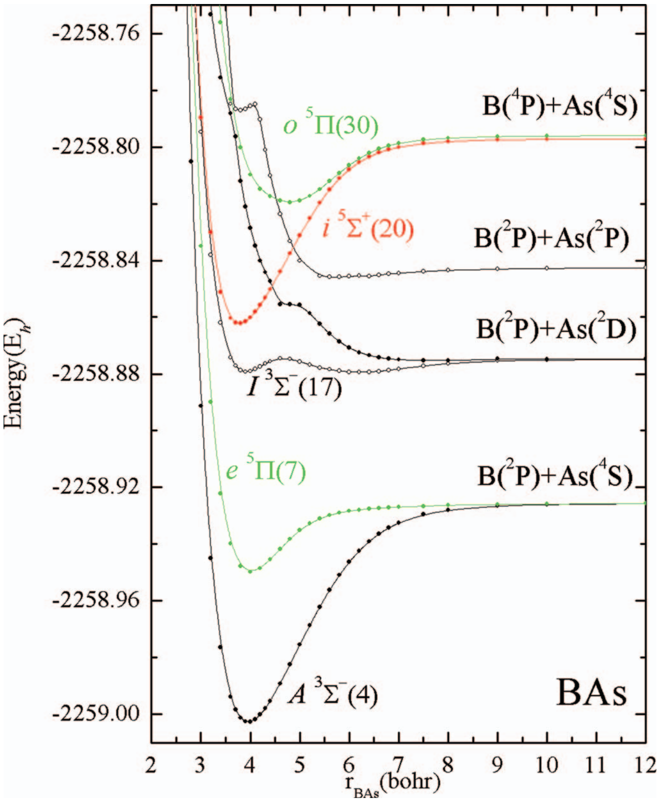

FIG. 5. MRCI/cc−pV5Z potential energy curves of the $A\ ^3\Sigma^-(4)$, $e\ ^5\Pi(7)$, $I\ ^3\Sigma^-(17)$, $i\ ^5\Sigma^+(20)$, and $o\ ^5\Pi(30)$ states.

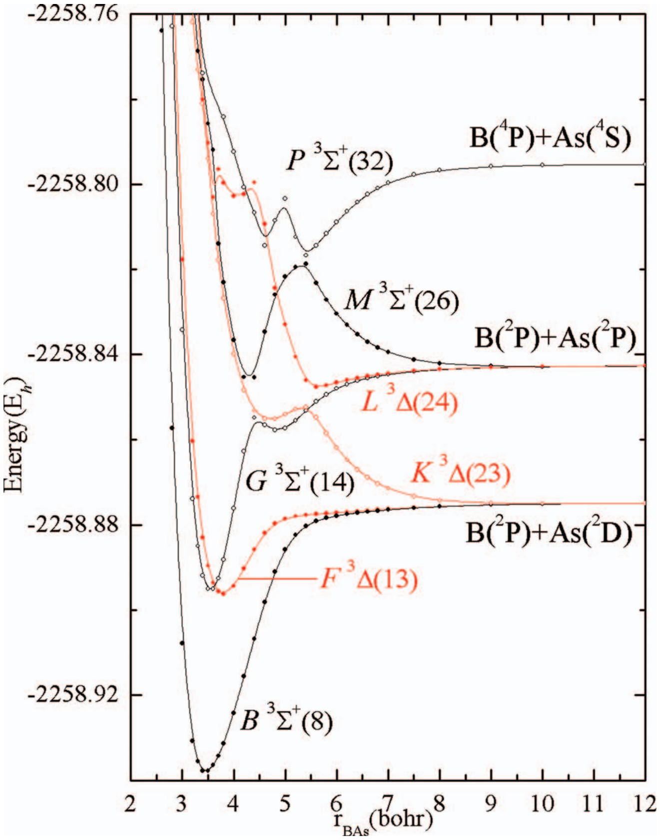

FIG. 6. MRCI/cc−pV5Z potential energy curves of the $B\ ^3\Sigma^+(8)$, $F\ ^3\Delta(13)$, $G\ ^3\Sigma^+(14)$, $K\ ^3\Delta(23)$, $L\ ^3\Delta(24)$, $M\ ^3\Sigma^+(26)$, and $P\ ^3\Sigma^+(32)$ states.

for both states. The bonding characteristics of the C and D $^3\Pi$ states are similar, a σ-bond is formed while along the π frame a charge transfer of ∼0.30e$^-$ from As to B takes place with a "back" transfer of ∼0.15e$^-$ from B to As, so the B atom is negatively charged by ∼0.15e$^-$. The minimum of the PEC is located at r$_e[C]$ = 2.100(2.105) Å and r$_e[D]$ = 2.090(2.094) Å with binding energies of D$_e[C]$ = 32.0(32.3) kcal/mol and D$_e[D]$ = 22.9(23.5) kcal/mol at the MRCI(+Q) level of theory. The $E\ ^3\Phi(11)$ state, sharing common asymptotic products $(|^2P,\ M_L = \pm 1\rangle_B \otimes |^2D,\ M_L = \pm 2\rangle_{As})$ with the $D\ ^3\Pi(10)$ state, has a completely parallel PEC to the D's one. It is characterized by a MRCI(+Q) value of r$_e$ = 2.119(2.119) Å and of D$_e$ = 20.2(21.2) kcal/mol.

The $H\ ^3\Pi(16)$ state entails the $As(^2D, M_L = \pm 1) = \{^{1/\sqrt{2}[|4s^2 4p_x^1 4p_y^2| - |4s^2 4p_x^1 4p_z^2|]}_{1/\sqrt{2}[|4s^2 4p_x^2 4p_y^1| - |4s^2 4p_y^1 4p_z^2|]}\}$ at infinity and is expected to be of repulsive character due to the incoming B(^{2}P, M$_L$ = 0) atom, and indeed this is the case; see Fig. 2. But an avoided crossing at around 4.4 bohr with the $J\ ^3\Pi(19)$ state originating from B(^{2}P, M$_L$ = ±1) + As(^{2}P, M$_L$ = 0) creates a rather shallow minimum at r$_e$ = 2.117 Å with D$_e$ = 3.1 kcal/mol (see Table I). The main CASSCF equilibrium configurations

$$|H^3\Pi(16)\rangle \approx \big|1\sigma^2 2\sigma^2 3\sigma^1\big[(0.81)1\pi_x^2 2\pi_x^1 + (0.44)1\pi_y^2 2\pi_x^1 + (0.26)1\pi_x^1 1\bar{\pi}_y^1 2\pi_y^1\big]\big\rangle$$

partially reflect its (J) asymptotic origin; $|As(^2P, M_L = 0)\rangle = |4s^2 4p_z^1(4p_x^2 + 4p_y^2)|$, while the Mulliken atomic distributions

$$2s^{1.41}2p_z^{0.59}2p_x^{0.92}2p_y^{0.17}(3d)^{0.06}/_B$$
$$4s^{1.82}4p_z^{1.01}4p_x^{1.41}4p_y^{0.48}(4d)^{0.12}/_{As},\ q_B = -0.15$$

indicate an *in situ* B atom in its excited ^{4}P state.

Three more states of $^3\Pi$ symmetry are displayed in Fig. 2, the J and N dissociating to B(^{2}P, $M_L = \pm1$, 0) + As(^{2}P, $M_L = 0$, ±1), respectively, and the O arising from the B(^{4}P, $M_L = \pm1$) + As(^{4}S) asymptotic channel. The $J\ ^3\Pi(19)$ state presents a MRCI(+Q) minimum at r_e = 2.198(2.178) Å with a D_e = 17.6(20.6) kcal/mol due to the above mentioned avoided crossing at ~4.4 bohr. The PEC of the $N\ ^3\Pi(29)$ state traces a repulsive path up to ~5.2 bohr due to the unfavorite electronic congestion along the σ-frame,

$$|^2P, M_L = 0\rangle_B \otimes |^2P, M_L = \pm1\rangle_{As} = \left|2s^2 2p_z^1\right| \otimes \left\{\begin{matrix} 1/\sqrt{2}\left[\left|4s^2 4p_x^2 4p_y^1\right| + \left|4s^2 4p_y^1 4p_z^2\right|\right] \\ 1/\sqrt{2}\left[\left|4s^2 4p_x^1 4p_y^2\right| + \left|4s^2 4p_x^1 4p_z^2\right|\right] \end{matrix}\right\}.$$

Its potential minimum is located at r_e = 2.356(2.289) Å and presents a barrier of ~5 (6) mE_h at the MRCI(+Q) level of theory, respectively (see Fig. 2). The last state to be mentioned is the $O\ ^3\Pi(31)$ one that arises from B(^{4}P) + As(^{4}S) and it is of vital importance since it transcends all other states of the same symmetry (*vide supra*). Its potential minimum is exactly on the top of the avoided crossing with the $N\ ^3\Pi(29)$ state at r_e = 2.836 Å (see Table I) and is bound by D_e = 13.6 kcal/mol.

B. $a\ ^1\Sigma^+(2)$, $d\ ^1\Sigma^+(6)$, $j\ ^1\Sigma^+(21)$, and $n\ ^1\Sigma^+(28)$

The first excited state of the BAs system is of $^1\Sigma^+$ symmetry and lies 8.5(7.7) kcal/mol above the $X\ ^3\Pi(1)$ state as is also the case in the BP system [$\Delta E(a\ ^1\Sigma^+ \leftarrow X\,^3\Pi)$ = 8 kcal/mol[3(d)]]. It originates from B(^{2}P, $M_L = \pm1$) + As(^{2}D, $M_L = \mp1$) and its asymptotic wavefunction reads

$$|^2P, M_L = \pm1\rangle_B \otimes |^2D, M_L = \mp1\rangle_{As} = \left\{\begin{matrix} \left|2s^2 2p_y^1\right| \\ \left|2s^2 2p_x^1\right| \end{matrix}\right\} \otimes \left\{\begin{matrix} 1/\sqrt{2}\left[\left|4s^2 4p_x^2 4p_y^1\right| - \left|4s^2 4p_y^1 4p_z^2\right|\right] \\ 1/\sqrt{2}\left[\left|4s^2 4p_x^1 4p_y^2\right| - \left|4s^2 4p_x^1 4p_z^2\right|\right] \end{matrix}\right\},$$

while at equilibrium the electronic character mirrors the $|^4P, M_L = 0\rangle_B \otimes |^4S\rangle_{As}$ asymptote, i.e.,

$$|a\,^1\Sigma^+(2)\rangle \approx 0.85\left|1\sigma^2 2\sigma^2 1\pi_x^2 1\pi_y^2\right\rangle + 0.22\left|1\sigma^2 2\sigma^2\left(1\pi_x^2 1\pi_y^1 2\bar{\pi}_y^1 + 1\pi_x^1 2\bar{\pi}_x^1 1\pi_y^2\right)\right\rangle,$$

where $1\sigma \sim (0.91)4s^{As} + (0.34)2s^B + (0.23)2p_z{}^B$, $2\sigma \sim (0.77)2s^B + (0.11)2p_z{}^B - (0.39)4s^{As} - (0.61)4p_z{}^{As}$, $1\pi \sim (0.84)4p_\pi{}^{As} + (0.45)2p_\pi{}^B$, $2\pi \sim (0.86)2p_\pi{}^B - (0.53)4p_\pi{}^{As}$ and Mulliken populations in conformity with the excited ^{4}P *in situ* B atom,

$$2s^{1.26}2p_z^{0.23}2p_x^{0.75}2p_y^{0.75}(3d)^{0.08}/_B$$
$$4s^{1.72}4p_z^{0.71}4p_x^{1.18}4p_y^{1.18}(4d)^{0.10}/_{As},\ q_B = -0.08.$$

All the above can be pictorially represented by the vbL diagram:

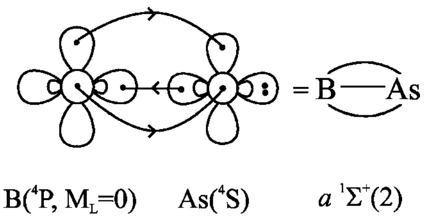

It is interesting to notice that the change of electronic character takes place after 4.4 bohr at which distance the a and $d\ ^1\Sigma^+$ states interact rather intensely; see Fig. 3. The minimum of the PEC is found at r_e = 1.788 Å and the binding energy value is D_e = 88.5 kcal/mol, both at the MRCI level of theory. The internal bond strength, i.e., the binding energy with respect to its diabatic end products is $D_e^{\text{diabatic}} = D_e^{\text{adiabatic}} + \Delta E[\text{B}(^4\text{P}) + \text{As}(^4\text{S}) \leftarrow \text{B}(^2\text{P}) + \text{As}(^2\text{D})]$ = 88.5 + 50.1 = 138.6 kcal/mol.

The formation of one σ and two π bonds is accompanied by a charge migration of ~0.5e$^-$ from B to As along the π-frame and a charge transfer of ~0.6e$^-$ from As to B via the σ route. Overall the B atom carries an excess of 0.1e$^-$ as is also the case in the $X\ ^3\Pi(1)$ state but the dipole moment vector is of opposite direction, i.e., $\mu_{ff}[a\ ^1\Sigma^+(2)] = -0.13$ D as contrasted to $\mu_{ff}[X\ ^3\Pi(1)] = 0.07$ D (see Table I).

The second and third states of $^1\Sigma^+$ symmetry, namely $d\ ^1\Sigma^+(6)$ and $j\ ^1\Sigma^+(21)$, correlate to B(^{2}P, $M_L = \pm1$,0) + As(^{2}P, $M_L = \mp1$,0), respectively, with asymptotic wavefunctions

$$|d\,^1\Sigma^+(6)\rangle = \left\{\begin{matrix} \left|2s^2 2p_y^1\right| \\ \left|2s^2 2p_x^1\right| \end{matrix}\right\} \otimes \left\{\begin{matrix} 1/\sqrt{2}\left[\left|4s^2 4p_x^2 4p_y^1\right| + \left|4s^2 4p_y^1 4p_z^2\right|\right] \\ 1/\sqrt{2}\left[\left|4s^2 4p_x^1 4p_y^2\right| + \left|4s^2 4p_x^1 4p_z^2\right|\right] \end{matrix}\right\}$$

and

$$\left|j\,^1\Sigma^+(21)\right\rangle \approx \left|2s^2 2p_z^1\right| \otimes 1/\sqrt{2}\left|4s^2 4p_z^1\left(4p_x^2 + 4p_y^2\right)\right|.$$

The minimum of the $d\ ^1\Sigma^+(6)$ state occurs at r_e = 2.056 (2.063) Å and is bound by D_e = 67.6(69.0) kcal/mol at the MRCI(+Q) level of theory. Its equilibrium CASSCF configurations,

$$\left|d\,^1\Sigma^+(6)\right\rangle \approx 0.65\left|1\sigma^2 2\sigma^2 3\sigma^2\left(1\pi_x^2 + 1\pi_y^2\right)\right\rangle,$$

clearly reflect the asymptotic origin of the $j\ ^1\Sigma^+(21)$ state due to a change of character at ~9.0 bohr. Along with the atomic populations

$$2s^{1.87}2p_z^{0.74}2p_x^{0.25}2p_y^{0.25}(3d)^{0.08}/_B$$
$$4s^{1.77}4p_z^{1.24}4p_x^{0.84}4p_y^{0.84}(4d)^{0.09}/_{As},\ q_B = -0.20,$$

we can unambiguously claim that B and As are connected by a σ and two putative π bonds exemplified by the following vbL diagram:

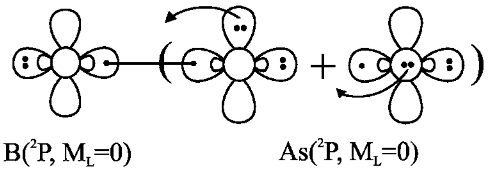

The $j\ ^1\Sigma^+(21)$ state presents a shallow local minimum at r = 3.058(2.996) Å at the MRCI(+Q) level of theory. Its electronic wavefunction has an intense multiconfiguration character making any prediction about its bonding characteristics difficult. This state would be uninteresting if it did not display an interesting topology (see Fig. 3) due to an avoided crossing with an incoming $^1\Sigma^+$ state $[n\,^1\Sigma^+(28)]$ originating from B(^{4}P) + As(^{4}S). Its global minimum occurs at r$_e$ = 1.767(1.789) Å with an adiabatic binding energy of D$_e$ = 10.4(14.5) kcal/mol, but its "true" or diabatic strength amounts to D$_e^{\text{diabatic}}$ = D$_e^{\text{adiabatic}}$ + ΔE[B(^{4}P) + As(^{4}S) ← B(^{2}P) + As(^{2}P)] = 10.4(14.5) + 29.8(32.5) = 40.2 (47.0) kcal/mol, at the MRCI(+Q) level of theory. Its main equilibrium CASSCF configurations,

$$|j^1\Sigma^+(21)\rangle \approx 0.76\left|1\sigma^2 2\sigma^1 3\bar{\sigma}^1 1\pi_x^2 1\pi_y^2\right\rangle$$
$$-0.35\left|1\sigma^2 2\sigma^2\left(1\pi_x^1 1\pi_y^2 2\bar{\pi}_x^1 + 1\pi_x^2 1\pi_y^1 2\bar{\pi}_y^1\right)\right\rangle,$$

where 1σ ~ (0.90)4s$^{\text{As}}$ + (0.37)2s$^{\text{B}}$ + (0.24)2p$_z{}^{\text{B}}$, 2σ ~ (0.76)2s$^{\text{B}}$ + (0.11)2p$_z{}^{\text{B}}$ – (0.41)4s$^{\text{As}}$ – (0.63)4p$_z{}^{\text{As}}$, 3σ ~ (0.43)2s$^{\text{B}}$ – (0.68)2p$_z{}^{\text{B}}$ + (0.64)4p$_z{}^{\text{As}}$, 1π ~ (0.84)4p$_\pi{}^{\text{As}}$ + (0.46)2p$_\pi{}^{\text{B}}$, 2π ~ (0.86)2p$_\pi{}^{\text{B}}$ – (0.53)4p$_\pi{}^{\text{As}}$ coupled to its Mulliken population analysis,

$$2s^{1.09}2p_z^{0.45}2p_x^{0.71}2p_y^{0.71}(3d)^{0.09}/_B$$
$$4s^{1.47}4p_z^{0.97}4p_x^{1.18}4p_y^{1.18}(4d)^{0.12}/_{As},\ q_B = -0.06,$$

point to an open singlet ($\frac{1}{2}$ σ, π_{x}, π_{y}) – bonded diradical, pictorially represented by

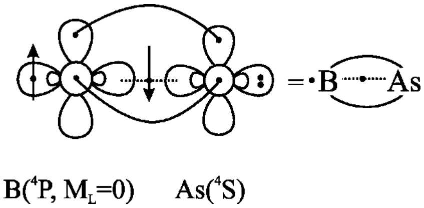

The last studied state of $^1\Sigma^+$ symmetry is the $n\,^1\Sigma^+(28)$ one dissociating to B(^{4}P) + As(^{4}S) and is responsible for the excited character of the *in situ* B atom in the previously discussed states (*vide supra*). Its PEC has a minimum just on the top of the avoided crossing with $j\,^1\Sigma^+(21)$ at r$_e$ = 2.49 Å with a strength of D$_e$ = 23.7 kcal/mol (see Table I). Its equilibrium wavefunction

$$|n^1\Sigma^+(28)\rangle \approx 0.59\left|1\sigma^2 2\sigma^2 3\sigma^2\left(1\pi_x^1 2\bar{\pi}_x^1 + 1\pi_y^1 2\bar{\pi}_y^1\right)\right\rangle$$
$$+0.23\left|1\sigma^2 2\sigma^2 3\sigma^1 4\bar{\sigma}^1\left(1\pi_x^2 + 1\pi_y^2\right)\right\rangle$$
$$+0.17\left|1\sigma^2 2\sigma^2 1\pi_x^2 1\pi_y^2\right\rangle$$

(1σ ~ 4s$^{\text{As}}$, 2σ ~ 2s$^{\text{B}}$, 3σ ~ 4p$_z{}^{\text{As}}$, 4σ ~ 2p$_z{}^{\text{B}}$, 1π ~ 4p$_\pi{}^{\text{As}}$, and 2π ~ 2p$_\pi{}^{\text{B}}$) is indeed an amalgam of resonant structures; the "0.59" CF originates from $|^2P;\ M_L = \pm1\rangle_B \otimes |^2P;\ M_L = \mp1\rangle_{As}$ while the "0.23" one from $|^2P;\ M_L = 0\rangle_B \otimes |^2P;\ M_L = 0\rangle_{As}$.

C. $c\,^1\Delta(5)$, $h\,^1\Delta(18)$, and $l\,^1\Delta(25)$

The $c\ ^1\Delta(5)$ and $h\ ^1\Delta(18)$ states correlate to B(^{2}P, M$_L$ = ±1,0) + As(^{2}D, M$_L$ = ±1, ±2) end products, respectively, so their asymptotic wavefunctions read

$$|c^1\Delta(5)\rangle = |^2P; M_L = \pm1\rangle_B \otimes |^2D; M_L = \pm1\rangle_{As}$$
$$= \left\{\begin{array}{l} \left|2s^2 2p_y^1\right| \\ \left|2s^2 2p_x^1\right| \end{array}\right\}$$
$$\otimes \left\{\begin{array}{l} {}^1\!/\!\sqrt{2}\left[\left|4s^2 4p_x^2 4p_y^1\right| - \left|4s^2 4p_y^1 4p_z^2\right|\right] \\ {}^1\!/\!\sqrt{2}\left[\left|4s^2 4p_x^1 4p_y^2\right| - \left|4s^2 4p_x^1 4p_z^2\right|\right] \end{array}\right\}$$

and

$$|h^1\Delta(18)\rangle = |^2P; M_L = 0\rangle_B \otimes |^2D; M_L = \pm 2\rangle_{As}$$
$$= |2s^2 2p_z^1| \otimes \left\{\begin{array}{l} {}^1\!/\!\sqrt{2}\left[\left|4s^2 4\bar{p}_x^1 4p_y^1 4p_z^1\right| - \left|4s^2 4p_x^1 4\bar{p}_y^1 4p_z^1\right|\right] \\ {}^1\!/\!\sqrt{2}\left[\left|4s^2 4p_x^2 4p_z^1\right| - \left|4s^2 4p_y^2 4p_z^1\right|\right] \end{array}\right\}.$$

These two $^1\Delta$ states interact at large distances (~9.0 bohr) and change their electronic character, thus the minimum of the $c\ ^1\Delta(5)$ state reflects in essence the asymptotic nature of the $h\ ^1\Delta(18)$ state. The CASSCF equilibrium configuration (A$_1$ component)

$$\left|c^1\Delta(5)\right\rangle \approx 0.67\left|1\sigma^2 2\sigma^2 3\sigma^2\left(1\pi_x^2 - 1\pi_y^2\right)\right\rangle$$

and its Mulliken analysis

$$2s^{1.90}2p_z^{0.79}2p_x^{0.19}2p_y^{0.19}(3d)^{0.08}/_B$$
$$4s^{1.80}4p_z^{1.27}4p_x^{0.84}4p_y^{0.84}(4d)^{0.09}/_{As}, q_B = -0.16$$

both point to a single σ and two putative π bonds graphically represented by the following vbL scheme:

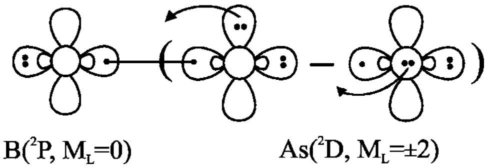

At this point we should notice the close similarity of the current $c\ ^1\Delta(5)$ state with the equilibrium character of the $d\ ^1\Sigma^+(6)$ state (*vide supra*) lying just 15.5(16.4) kcal/mol higher (see Table I), their only difference being a sign "+" $[d\,^1\Sigma^+(6)]$ /"−" $[c\,^1\Delta(5)]$ in their CASSCF equilibrium configurations. This bonding similarity is also reflected at the MRCI(+Q) equilibrium distances r$_e$[$c\,^1\Delta(5)$] = 2.089(2.086) Å versus r$_e$[$d\,^1\Sigma^+(6)$] = 2.056(2.063) Å and adiabatic binding energy values of D$_e$[$c^1\Delta(5)$] = 62.9(64.2) *vs* D$_e$[$d^1\Sigma^+(6)$] = 67.6(69.0) kcal/mol. We should remind though that the equilibrium character of the $d\,^1\Sigma^+(6)$ state is essentially that of the asymptotic origin of the $j^1\Sigma^+(21)$ one, i.e., B(^{2}P, M$_L$ = 0) + As(^{2}P, M$_L$ = 0) or in terms of real orbitals $|2s^2 2p_z^1| \otimes |4s^2 4p_z^1 1/\sqrt{2}(4p_x^2 + 4p_y^2)|$.

The remaining two $^1\Delta$ states, the h and l, originate from B(^{2}P, M$_L$ = 0) + As(^{2}D, M$_L$ = ±2) (but see above) and B(^{2}P, M$_L$ = ±1) + As(^{2}P, M$_L$ = ±1), respectively, and are rather uninteresting presenting two and one shallow minima, respectively (see Table I and Fig. 3).

D. $g\,^1\Sigma^-(15)$, $k\,^1\Sigma^-(22)$, and $m\,^1\Sigma^-(27)$

The g and k $^1\Sigma^-$ states correlate to B(^{2}P, M$_L$ = ±1,0) + As(^{2}D, M$_L$ = ∓1,0), respectively, while the m $^1\Sigma^-$ state correlates to the B(^{2}P, M$_L$ = ±1) + As(^{2}P,M$_L$ = ∓1) fragments. The g $^1\Sigma^-(15)$ state presents a rather shallow minimum at r$_e$ = 2.05(2.05) Å with a D$_e$ = 3.9(6.7) kcal/mol at the MRCI(+Q) level of theory. It is also interesting to notice the resemblance of the g and h PECs (see Fig. 3) mainly due to their same end products $|^2P; M_L = \pm 1\rangle_B \otimes |^2D; M_L = \mp 1(g), \pm 1(h)\rangle_{As}$. The k $^1\Sigma^-(22)$ state originates from the B(^{2}P, M$_L$ = 0) + As(^{2}D, M$_L$ = 0) asymptotic channel and its wavefunction at infinity reads

$$|k\,^1\Sigma^-(22)\rangle \approx \left|2s^2 2p_z^1\right| \otimes 1/\sqrt{6}\big[2\left|4s^2 4p_x^1 4p_y^1 4\bar{p}_z^1\right| - \left|4s^2 4p_x^1 4\bar{p}_y^1 4p_z^1\right| - \left|4s^2 4\bar{p}_x^1 4p_y^1 4p_z^1\right|\big].$$

The repulsive character of this state can be rationalized on the basis of the above expression. The spin coupling of $|^2D;\, M_L = 0\rangle_{As}$ does not offer a fruitful interaction with an incoming B(^{2}P, M$_L$ = 0) atom, but an avoided crossing with the m $^1\Sigma^-(27)$ state at ∼5.4 bohr creates a local minimum. The electronic character at the MRCI(+Q) minimum of r$_e$ = 2.421(2.352) Å is completely due to

$$|^2P; M_L = \pm 1\rangle_B \otimes |^2P; M_L = \mp 1\rangle_{As} = \left\{\begin{matrix} \left|2s^2 2p_y^1\right| \\ \left|2s^2 2p_x^1\right| \end{matrix}\right\} \otimes \left\{\begin{matrix} {}^1\!/\!\sqrt{2}\left[\left|4s^2 4p_y^1 4p_x^2\right| + \left|4s^2 4p_y^1 4p_z^2\right|\right] \\ {}^1\!/\!\sqrt{2}\left[\left|4s^2 4p_x^1 4p_y^2\right| + \left|4s^2 4p_x^1 4p_z^2\right|\right] \end{matrix}\right\}.$$

The m $^1\Sigma^-(27)$ state and just because of the above mentioned avoided crossing shows a tiny attractive behavior, but it is essentially a continuation of the repulsive nature of the k $^1\Sigma^-(22)$ PEC.

At this point we should say a few words about the similarities/dissimilarities found in the PECs of the a $^1\Sigma^+(2)$, j $^1\Sigma^+(21)$, g $^1\Sigma^-(15)$, m $^1\Sigma^-(27)$, h $^1\Delta(18)$, and $l^1\Delta(25)$ states. All of them share similar end products, i.e.,

$$|a, g, h\rangle \sim |^2P; M_L = \pm 1\rangle_B \otimes |^2D; M_L = \mp 1, \mp 1, \pm 1\rangle_{As},$$

$$|j, l, m\rangle \sim |^2P; M_L = \pm 1\rangle_B \otimes |^2P; M_L = \mp 1, \pm 1, \mp 1\rangle_{As},$$

but not all PECs display the same features (see Fig. 3). The g and h states are slightly bound but the a state is strongly bound although all of them result from a quasi-identical atomic combination.

The same also holds for the j (local) (but see above) and l states. The "attractiveness" of the a state even at large distances results from the intense interaction with primarily the d state and secondary with the n $^1\Sigma^+(28)$ state due to the σ and π bonds that can be formed (*vide supra*). Due to symmetry reasons this cannot be the case for the g, h, j (local) and l states.

E. $b\,^1\Pi(3)$, $f\,^1\Pi(12)$, and $p\,^1\Pi(33)$

There are three states of Π and one of Φ spatial symmetry arising from the B(^{2}P) + As(^{2}D) dissociation limit of singlet and triplet spin multiplicity. All four triplet states are bound with respect to their adiabatic end products (see Fig. 2) but only two $^1\Pi$ states are bound, the rest being of repulsive character, see Fig. 4. The b $^1\Pi(3)$ and f $^1\Pi(12)$ states emanate from $|^2P; M_L = \pm 1\rangle_B \otimes |^2D; M_L = 0, \mp 2\rangle_{As}$, respectively, and present their MRCI(+Q) minima at r$_e(b)$ = 1.879(1.878) Å and r$_e(f)$ = 2.132(2.154) Å with MRCI(+Q) binding energies D$_e(b)$ = 87.9(88.1) kcal/mol and D$_e(f)$ = 17.6(19.4) kcal/mol. Their triplet analogues are the C $^3\Pi(9)$ and D $^3\Pi(10)$ states while the E $^3\Phi(11)$ state being completely isomorphous to the D state strangely enough does not have a singlet analogue. Their asymptotic wavefunctions read

$$|b\rangle = \left\{\begin{matrix} \left|2s^2 2p_y^1\right| \\ \left|2s^2 2p_x^1\right| \end{matrix}\right\} \otimes {}^1\!/\!\sqrt{6}\big[2\left|4s^2 4p_x^1 4p_y^1 4\bar{p}_z^1\right| - \left|4s^2 4p_x^1 4\bar{p}_y^1 4p_z^1\right| - \left|4s^2 4\bar{p}_x^1 4p_y^1 4p_z^1\right|\big]$$

and

$$|f\rangle = \left\{\begin{matrix} \left|2s^2 2p_y^1\right| \\ \left|2s^2 2p_x^1\right| \end{matrix}\right\} \otimes \left\{\begin{matrix} {}^1\!/\!\sqrt{2}\left[\left|4s^2 4p_z^1 4p_x^1 4\bar{p}_y^1\right| - \left|4s^2 4p_z^1 4\bar{p}_x^1 4p_y^1\right|\right] \\ {}^1\!/\!\sqrt{2}\left[\left|4s^2 4p_z^1 4p_x^2\right| - \left|4s^2 4p_z^1 4p_y^2\right|\right] \end{matrix}\right\},$$

while at equilibrium they are

$$|b\rangle \approx 0.92\left|1\sigma^2 2\sigma^2 3\sigma^1 1\bar{\pi}_x^1 1\pi_y^2\right| + 0.24\left|1\sigma^2 2\sigma^2 3\sigma^1 1\bar{\pi}_x^1 1\pi_y^1 2\bar{\pi}_y^1\right|$$

and

$$|f\rangle \approx 0.66\left|1\sigma^2 2\sigma^2 3\sigma^1 1\pi_x^1 1\bar{\pi}_y^1 2\bar{\pi}_y^1\right| - 0.39\left|1\sigma^2 2\sigma^2 3\sigma^1 1\pi_y^2 2\bar{\pi}_x^1\right| + 0.37\left|1\sigma^2 2\sigma^2 3\sigma^1 1\bar{\pi}_x^1 1\pi_y^1 2\bar{\pi}_y^1\right| - 0.31\left|1\sigma^2 2\sigma^2 3\sigma^1 1\bar{\pi}_x^1 1\pi_y^2\right|.$$

b's state Mulliken atomic populations,

$$2s^{1.39} 2p_z^{0.67} 2p_x^{0.19} 2p_y^{0.69} (3d)^{0.09}/_B$$

$$4s^{1.76} 4p_z^{1.02} 4p_x^{0.79} 4p_y^{1.23} (4d)^{0.12}/_{As},\ q_B = -0.06,$$

coupled to the "0.92" component of its equilibrium wavefunction reveal a rather clean bonding situation represented by the below vbL scheme

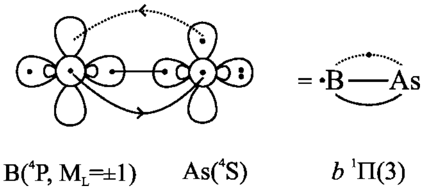

featuring one σ, one and a half π bonds. It is interesting to remind at this point that the triplet analogue of the b's "0.92" component is only "0.46" and that explains the large difference in the binding energies; D$_e(b)$ = 87.9 kcal/mol *vs* $D_e(C) = 32.0$ kcal/mol. The *b* state is "localized" on a nicely bonded structure whereas its triplet *C* state is "dispersed" on at least three structures (*vide supra*). The $f\,^1\Pi(12)$ and $D\,^3\Pi(10)$ states are equally dispersed on different determinants and are consequently energetically close, they differ by $\sim 8mE_h$. The last studied $^1\Pi$ state results from the B(^{4}P, $M_L = \pm1$) +As(^{4}S) excited limit. Its potential minimum is due to an avoided crossing with the $^1\Pi$ state (not tagged in Fig. 4) arising from B(^{2}P, $M_L = 0$) + As(^{2}P, $M_L = \pm1$). We should notice at this point the close resemblance of this pair of $^1\Pi$ states with the $N\,^3\Pi(29)$ and $O\,^3\Pi(31)$ ones (see Fig. 2). They have the same asymptotic end products and similar morphology. Their only difference is the lack of a local minimum in the PEC of the singlet analogue of the $N\,^3\Pi(29)$ state.

F. $A\,^3\Sigma^-(4)$ and $I\,^3\Sigma^-(17)$

The $A^3\Sigma^-(4)$ state results from the ground state fragments B(^{2}P, $M_L = 0$) + As(^{4}S). The atomic combination mode is such that it facilitates the formation of a σ and two half π bonds. Both the equilibrium CF and Mulliken population analysis

$$|A^3\Sigma^-(4)\rangle \approx 0.93\,\left|1\sigma^2 2\sigma^2 3\sigma^2 1\pi_x^1 1\pi_y^1\right\rangle$$

and

$$2s^{1.87}2p_z^{0.83}2p_x^{0.15}2p_y^{0.15}(3d)^{0.07}/_B$$

$$4s^{1.82}4p_z^{1.24}4p_x^{0.88}4p_y^{0.88}(4d)^{0.08}/_{As},\ q_B = -0.09$$

can be visualized by the following vbL scheme:

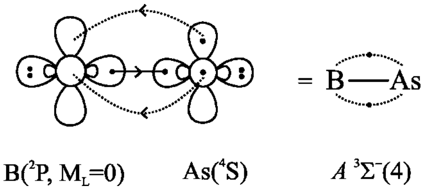

The formation of the σ bond is accompanied by a charge migration of $\sim 0.2e^-$ along the σ-frame from B to As while $\sim 0.3e^-$ are transferred from As to B via the π route.

Three more states of $^3\Sigma^-$symmetry are issued from B(^{2}P, $M_L = \pm1, 0$) + As(^{2}D, $M_L = \mp1, 0$) and B(^{2}P, $M_L = \pm1$) + As(^{2}P, $M_L = \mp1$) but as can be seen in Fig. 5 are quite uninteresting. The lowest of them, $I^3\Sigma^-(17)$, correlates to $|^2P;\ M_L = \pm1\rangle_B \otimes |^2D;\ M_L = \mp1\rangle_{As}$ and presents two practically degenerate shallow minima at r = 3.28 and 2.07 Å worthing ~2.8 kcal/mol (see Table I).

G. $e\,^5\Pi(7)$, $o\,^5\Pi(30)$, and $i\,^5\Sigma^+(20)$

There are in total four quintet states arising from B(^{2}P, ^{4}P) + As(^{4}S) of Σ^+, Σ^-, and Π[2] spatial symmetries. The $^5\Sigma^-$ is of repulsive character due to its asymptotic combination mode; $|^5\Sigma^-\rangle = |2s^2 2p_z^1\rangle_B \otimes |4s^2 4p_x^1 4p_y^1 4p_z^1\rangle_{As}$ while the other three quintet states are well bound. The $e\,^5\Pi(7)$ state (see Fig. 5) is bound by $D_e = 15.1$ (16.2) kcal/mol at $r_e = 2.111(2.111)$ Å at the MRCI(+Q) level of theory. Its equilibrium CASSCF configuration along with its Mulliken atomic population,

$$|e^5\Pi(7)\rangle \approx 0.96\,\left|1\sigma^2 2\sigma^2 3\sigma^1 1\pi_x^1 1\pi_y^1 2\pi_y^1\right\rangle,$$

where $1\sigma \sim 4s^{As}$, $2\sigma \sim (0.65)2s^B + (0.23)2p_z{}^B - (0.27)4s^{As} - (0.68)4p_z{}^{As}$, $3\sigma \sim (0.69)2s^B - (0.51)2p_z{}^B + (0.58)4p_z{}^{As}$, $1\pi \sim (0.39)2p_\pi{}^B + (0.87)4p_\pi{}^{As}$, $2\pi \sim (0.85)2p_\pi{}^B - (0.53)4p_\pi{}^{As}$ and

$$2s^{1.47}2p_z^{0.55}2p_x^{0.14}2p_y^{0.96}(3d)^{0.05}/_B$$

$$4s^{1.84}4p_z^{1.0}4p_x^{0.87}4p_y^{0.98}(4d)^{0.12}/_{As},\ q_B = -0.17,$$

point to a partially excited B(^{4}P) atom that can form a σ and a half π bonds with As(^{4}S). The above can be cast in the following pictorial representation:

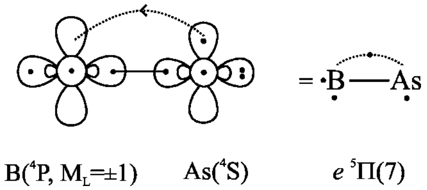

The σ bond is made possible through the formation of two rather pronounced sp_z hybrids on B while a $\sim 0.14e^-$ charge migration from As to B via the π route adds to the energy stabilization.

The second $o\,^5\Pi(30)$ state is of essentially the same character. Its equilibrium configurations

$$|o^5\Pi(30)\rangle \approx 0.75\,\left|1\sigma^2 2\sigma^1 3\sigma^2 1\pi_x^1 1\pi_y^1 2\pi_y^1\right\rangle$$
$$- 0.49\,\left|1\sigma^2 2\sigma^2 4\sigma^1 1\pi_x^1 1\pi_y^1 2\pi_y^1\right\rangle$$

and atomic distributions

$$2s^{1.22}2p_z^{0.66}2p_x^{0.16}2p_y^{0.98}(3d)^{0.05}/_B$$

$$4s^{1.89}4p_z^{1.1}4p_x^{0.86}4p_y^{0.99}(4d)^{0.09}/_{As},\ q_B = -0.07$$

reveal a similar bonding pattern as above. This is also corroborated by the same adiabatic binding energy $D_e = 14.7(17.5)$ kcal/mol and identical dipole moment values $\langle\mu\rangle = 0.92$ D (see Table I).

The $i\,^5\Sigma^+(20)$ state arises from B(^{4}P, $M_L = 0$) + As(^{4}S) and its wavefunction at infinity reads

$$\begin{aligned}|i^5\Sigma^+(20)\rangle \approx\ & \left|4s_{As}^2\left(4p_z^1 2s_B^1\right)_S 4p_x^1 4p_y^1 2p_x^1 2p_y^1\right| \\ & + \left|4s^2 4p_z^1 2s_B^1\left(4p_x^1 2p_x^1\right)_S 4p_y^1 2p_y^1\right| \\ & + \left|4s^2 4p_z^1 2s_B^1 4p_x^1 2p_x^1\left(4p_y^1 2p_y^1\right)_S\right|,\end{aligned}$$

where the symbol $(\ldots)_S$ means that the electrons within parentheses are singly coupled with the remaining ones being high spin coupled. The above form adds a "bonding" flexibility and this explains perhaps its greater stability than that of the $^5\Pi$ (*e* and *o*) symmetry; $D_e[i\,^5\Sigma^+(20)] = 40.9$ kcal/mol *vs* $D_e(e \text{ or } o) \approx 16$ kcal/mol (see Table I). The equilibrium configurations are essentially identical in character to the ones at infinity while the Mulliken atomic distributions,

$$2s^{1.06}2p_z^{0.48}2p_x^{0.81}2p_y^{0.81}(3d)^{0.07}/_B$$

$$4s^{1.70}4p_z^{0.67}4p_x^{1.11}4p_y^{1.11}(4d)^{0.13}/_{As},\ q_B = -0.24,$$

enable us to draw the following bonding scheme:

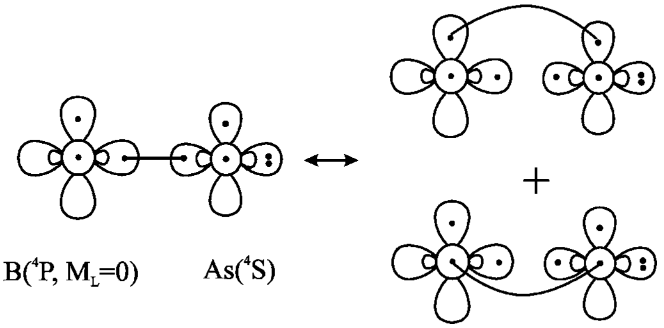

which is actually a hybrid between a σ- and a π-bonded chemical structures. Overall ∼0.4e$^-$ are transferred from B to As through the π-frame and ∼0.6e$^-$ are back transferred through the σ frame thus creating an electronic excess on B.

H. *B* $^3\Sigma^+$(8), *G* $^3\Sigma^+$(14), *M* $^3\Sigma^+$(26), and *P* $^3\Sigma^+$(32)

The *B*, *G*, *M*, and *P* $^3\Sigma^+$ states correlate to B(^{2}P, M$_L$ = ±1) + As(^{2}D, M$_L$ = ∓1), B(^{2}P, M$_L$ = 0,±1) + As(^{2}P, M$_L$ = 0,∓1), and B(^{4}P, M$_L$ = 0) + As(^{4}S), respectively, and their potential curves, displayed in Fig. 6, show a strong interplay due to the "furious" *P* diabate correlating to B(^{4}P) + As(^{4}S).

The equilibrium character of the *B* $^3\Sigma^+$(8) state is a hybrid of two resonant structures,

$$|B^3\Sigma^+(8)\rangle \approx 0.59\left|1\sigma^2 2\sigma^1 3\sigma^1 1\pi_x^2 1\pi_y^2\right\rangle + 0.49\left|1\sigma^2 2\sigma^2\left(1\pi_x^2 1\pi_y^1 2\pi_y^1 + 1\pi_x^1 2\pi_x^1 1\pi_y^2\right)\right\rangle,$$

with the "0.59" component characterizing the B(^{4}P) + As(^{4}S) diabate while the "0.49" one reflects the electronic distribution of its adiabatic origin.

The *G* and *M* $^3\Sigma^+$ states both correlate to the same asymptote. They exchange their character at ∼9.0 bohr so the local minimum at ∼4.8 bohr of the *G* PEC mirrors in essence the $|^2P, M_L = \pm 1\rangle_B \otimes |^2P, M_L = \mp 1\rangle_{As}$ character while the *M* state is repulsive due to the $|2s^2 2p_z^1| \otimes |4s^2 4p_z^1(4p_x^2 + 4p_y^2)|$ electronic distribution. It is interesting to remind at this place that the *M* state (up to 5.4 bohr) is the triplet analogue of the *d* $^1\Sigma^+$(6) state (see Fig. 3) that is strongly bound by ∼68 kcal/mol (see Table I). The *M* PEC suffers an avoided crossing with the *P* $^3\Sigma^+$ state originating from B(^{4}P) + As(^{4}S) at 5.4 bohr and assumes an attractive character (see Fig. 6). That "attractiveness" stops rather abruptly at ∼4.3 bohr due to another avoided crossing with the *G* curve, while the [B(^{4}P) + As(^{4}S)] behavior is transferred to the global minimum of the *G* state at r$_e$ = 1.878 Å with a D$_e$ = 33.1 kcal/mol but clearly its "diabatic" strength is $D_e^{\text{diabatic}} = D_e^{\text{adiabatic}} + \Delta E[\text{B}(^4\text{P}) + \text{As}(^4\text{S}) \leftarrow \text{B}(^2\text{P}) + \text{As}(^2\text{P})] = 33.1 + 29.7 = 62.8$ kcal/mol. The *G*, *M*, and *P* adiabatic curves are so intermingled that the Born−Oppenheimer approximation breaks down so blatantly that a safe way to find the vibrational levels of the $^3\Sigma^+$ manifold at energies E > E$_e$[*G* $^3\Sigma^+$(14)] would be only through a vibronic coupling approach.

I. *F* $^3\Delta$(13), *K* $^3\Delta$(23), and *L* $^3\Delta$(24)

There are two $^3\Delta$ states dissociating to B(^{2}P) + As(^{2}D) with the $|^2P, M_L = \pm 1\rangle_B \otimes |^2D, M_L = \pm 1\rangle_{As}$ and $|^2P, M_L = 0\rangle_B \otimes |^2D, M_L = \pm 2\rangle_{As}$ combination modes. The second one, (0, ±2), results in a repulsive curve due to the high spin (4p$_z^1$ – 2p$_z^1$) interaction between the two approaching atoms (but see below). The (±1, ±1) combination mode results in an attractive curve that is bound by 13.4 kcal/mol. The equilibrium configuration

$$|F^3\Delta(13)\rangle \approx 0.65\left|1\sigma^2 2\sigma^2\left(1\pi_x^1 2\pi_x^1 1\pi_y^2 - 1\pi_x^2 1\pi_y^1 2\pi_y^1\right)\right\rangle,$$

along with the atomic populations

$$2s^{1.38} 2p_z^{0.18} 2p_x^{0.74} 2p_y^{0.74} (3d)^{0.07}/_B$$

$$4s^{1.79} 4p_z^{0.57} 4p_x^{1.18} 4p_y^{1.18} (4d)^{0.13}/_{As},\ q_B = -0.12,$$

point to the following bonding scheme.

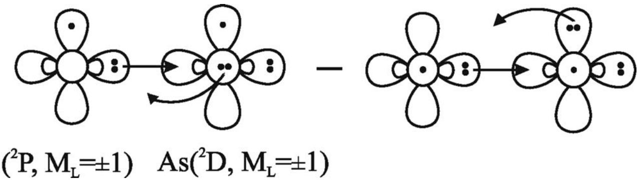

showing two putative bonds, a σ and a π

The *K* $^3\Delta$(23) state being repulsive due to the Pauli wall between the high spin 4p$_z^1$ – 2p$_z^1$ electrons suffers an avoided crossing at ∼5.4 bohr (see Fig. 6) with the incoming *L* $^3\Delta$(24) state which is very similar in character with the *F* $^3\Delta$(13) state. Its equilibrium configurations,

$$|K^3\Delta(23)\rangle \approx 0.57\left|1\sigma^2 2\sigma^2 3\sigma^2\left(1\pi_x^1 2\pi_x^1 - 1\pi_y^1 2\pi_y^1\right)\right\rangle + 0.34\left|1\sigma^2 2\sigma^2\left(1\pi_x^1 2\pi_x^1 1\pi_y^2 - 1\pi_x^2 1\pi_y^1 2\pi_y^1\right)\right\rangle,$$

is just a transfer of the asymptotic $|^2P, M_L = \pm 1\rangle_B \otimes |^2P, M_L = \pm 1\rangle_{As}$ character at the equilibrium distance r$_e$ = 2.492 Å of the *K* state.

The *L* state shows an attraction of ∼3 kcal/mol at r$_e$ ∼ 2.98 Å just because of its interaction with *K*.

IV. CONCLUSIONS

We offer for the first time a detailed *ab initio* study of the diatomic molecule BAs. MRCI/cc−pV5Z potential energy curves have been constructed for 42 $^{2S+1}\Lambda$ states dissociating to the first four asymptotic end channels. Thirty three states are either bound or present local minima while the remaining nine states are purely repulsive.

The morphology of the PECs reveals a rich spectroscopy where perturbations due to non-adiabatic effects should be the rule than the exception. Numerous avoided crossings appear on more or less all studied states but the most pronounced ones entail the $^{1,3}(\Sigma^+, \Pi)$ states arising from B(^{4}P) + As(^{4}S).

The ground state is of $^3\Pi$ symmetry in line with the isovalent diatomics BN and BP. It dissociates adiabatically to the ground state fragments, i.e., B(^{2}P) + As(^{4}S), while at equilibrium the B atom is found in its excited ^{4}P state. The binding energy is D$_e$ = 65.24(66.3) kcal/mol at r$_e$ = 1.869(1.870) Å at the MRCI(+Q) level of theory. Its first excited *a* $^1\Sigma^+$(2)

state lies $T_e = 8.5(7.7)$ kcal/mol higher and features three full bonds, one σ and two π with a $D_e = 88.53(88.7)$ kcal/mol at $r_e = 1.788(1.788)$ Å at the MRCI(+Q) level. The second excited state, $b\,^1\Pi(3)$, quasi-degenerate to $a\,^1\Sigma^+(2)$, is the singlet analogue of the $X\,^3\Pi(1)$ state. The binding mode remains essentially the same but the spin flip elongates the distance by 0.01 Å.

We believe that the present work fills the gap of the theoretical investigation of the diatomics of B with elements of the VA group and we hope that it will initiate an experimental investigation.

[1] J. A. Perri, S. LaPlaca, and B. Post, Acta Cryst. **11**, 310 (1958).

[2] D. J. Stukel, Phys. Rev. B **1**, 3458 (1970); T. L. Chu and A. E. Hyslop, J. Appl. Phys. **43**, 276 (1972); C. Prasad and M. Sahay, Phys. Status Solidi B **154**, 201 (1989); G. L. W. Hart and A. Zunger, Phys. Rev. B **62**, 13522 (2000); R. Ahmed, S. J. Hashemifar, H. Akbarzadeh, M. Ahmed, and F.- e-Aleem, Comput. Mater. Sci. **39**, 580 (2007); X. De-Ping, Z. Shou-Li, W. Qi, and R. Xiao-Min, Chin. Phys. B **17**, 3062 (2008); S. Bağci, S. Duman, H. M. Tütüncü, and G. P. Srivastava, Phys. Rev. B **79**, 125326 (2009); S. Cui, W. Feng, H. Hu, Z. Feng, and Y. Wang, Compt. Mat. Sci. **44**, 1386 (2009); R. Mohammad, and S. Katırcıoğlu, J. Alloys Compd. **485**, 687 (2009); A. Boudjemline, M. M. Islam, L. Louail, and B. Diawara, Physica B **406**, 4272 (2011); L. Zhi-Feng, L. Xue-Ling, L. Li-Ren, L. Huo-Yan, and Z. Heng-Jiang, Chin. Phys. B **20**, 023101 (2011); S. Wang, S. F. Swingle, H. Ye, F.-R. F. Fan, A. H. Cowley, and A. J. Bard, J. Am. Chem. Soc. **134**, 11056 (2012).

[3] (a) J. M. L. Martin, T. J. Lee, G. E. Scuseria, and P. R. Taylor, J. Chem. Phys. **97**, 6549 (1992); (b) C. W. Bauschlicher, Jr. and H. Partridge, Chem. Phys. Lett. **257**, 601 (1996); (c) A. Kalemos, T. H. Dunning, Jr., and A. Mavridis, J. Chem. Phys. **120**, 1813 (2004); (d) Z. Gan, D. J. Grant, R. J. Harrison, and D. A. Dixon, *ibid.* **125**, 124311 (2006); (e) A. Karton and J. M. Martin, *ibid.* **125**, 144313 (2006); (f) X. Li and J. Paldus, Chem. Phys. Lett. **431**, 179 (2006); (g) X. Li, J. R. Gour, J. Paldus, and P. Piecuch, Chem. Phys. Lett. **461**, 321 (2008); (h) D. Shi, W. Xing, H. Liu, J. Sun, Z. Zhu, and Y. Liu, Spectrochim. Acta, Part A **93**, 367 (2012).

[4] (a) A. I. Boldyrev and J. Simons, J. Phys. Chem. **97**, 6149 (1993); (b) B. Miguel, S. Omar, P. Mori-Sánchez, and J. M. García de la Vega, Chem. Phys. Lett. **381**, 720 (2003); (c) R. Linguerri, N. Komiha, R. Oswald, A. Mitrushchenkov, and P. Rosmus, Chem. Phys. **346**, 1 (2008).

[5] K. R. Asmis, T. R. Taylor, and D. M. Neumark, Chem. Phys. Lett. **295**, 75 (1998).

[6] A. Kramida, Yu. Ralchenko, J. Reader and NIST ASD Team, NIST Atomic Spectra Database, version 5.0, National Institute of Standards and Technology, Gaithersburg, MD , 2012, see http://physics.nist.gov/asd (accessed April 11, 2013).

[7] C. F. Bunge, J. A. Barrientos, and A. V. Bunge, At. Data Nucl. Data Tables **53**, 113 (1993).

[8] (a) T. H. Dunning, Jr., J. Chem. Phys. **90**, 1007 (1989); (b) A. K. Wilson, D. E. Woon, K. A. Peterson, and T. H. Dunning, Jr., *ibid.* **110**, 7667 (1999); (c) W. A. de Jong, R. J. Harrison, and D. A. Dixon, *ibid.* **114**, 48 (2001).

[9] H.-J. Werner, P. J. Knowles, G. Knizia, F. R. Manby, M. Schütz, *et al.*, MOLPRO, version 2010.1, a package of *ab initio* programs, 2010, see http://www.molpro.net